Two-pion production in deuteron-deuteron collisions at low energies

G. Fäldt[1,a], U. Tengblad[1,b], and C. Wilkin[2,c]

[1] Department of Radiation Sciences, Box 535, S-751 21 Uppsala, Sweden
[2] Department of Physics & Astronomy, UCL, London WC1E 6BT, UK

Abstract. The cross-section for the $dd \to {}^4\text{He}\,\pi\pi$ reaction is estimated near threshold in a two-step model where a pion created in a first interaction produces a second pion in a subsequent interaction. This approach, which describes well the rates of 2π and η production in the $pd \to {}^3\text{He}\,\pi\pi$ and $dd \to {}^4\text{He}\,\eta$ reactions, leads to predictions that are much too low compared to experiment. Alternatives to this and the double-Δ model will have to be sought to explain these data.

PACS. 13.60.Le Meson production – 14.40.Aq π, K, and η mesons

1 Introduction

Over the last few years there has been increased experimental interest in double-pion production near threshold in several hadronic reactions. These include studies in pion-proton [1] and proton-proton collisions [2], as well as in the $pd \to {}^3\text{He}\,\pi\pi$ [3–5] and $dd \to {}^4\text{He}\,\pi\pi$ [6–8] reactions. For excess energies Q below about 100 MeV one sees no sign of the low-mass s-wave $\pi\pi$ enhancement, known as the ABC effect [9], and the maxima in the invariant mass distributions tend more to be pushed to the highest possible values.

Due in part to an isospin filter effect, the most spectacular manifestation of the ABC is to be found in the case of $dd \to {}^4\text{He}\,\pi\pi$ for $Q \approx 200$–300 MeV [10]. These cross-section data, as well those representing the deuteron analysing powers [11], can be well understood within a model where there are two independent pion productions, through the $pn \to d\pi^0$ reaction, with a final-state interaction between the two deuterons to yield the observed α-particle [12]. Since the $pn \to d\pi^0$ amplitudes are dominated by p-wave production, driven by the Δ isobar, this leads to much structure in the predictions. Although such double-Δ effects are generally observed in the medium energy data [10,12], there is little evidence of them nearer to threshold [6,7,13]. Furthermore, the cross-sections measured at low energies are over an order of magnitude higher than the predictions of models behaving like the square of

p-wave production, where the amplitudes must be proportional to Q.

In an alternative approach to the $pd \to {}^3\text{He}\,\pi\pi$ reaction, the low-energy cross-sections have been discussed in terms of a two-step model, where a pion is produced through a $pp \to d\pi^+$ reaction on the proton in the deuteron, with a further pion being created in a secondary $\pi^+ n \to p\pi^0\pi^0$ reaction [14]. There are, of course, other contributions related to this through isospin invariance. Semi-phenomenological models of the $\pi^+ n \to p\pi^0\pi^0$ amplitudes show strong s-wave production, behaving rather like a contact term, plus another contribution involving the decay chain $N^*(1440) \to \Delta(1232)\,\pi \to N\pi\pi$ [15]. The s-wave term is sufficient, in the two-step model, to lead to reasonable agreement with the available data on the $pd \to {}^3\text{He}\,\pi\pi$ total cross-section. Moreover, combined with p-waves required by the decay chain, it reproduces the shift of the mass spectrum away from the ABC region towards that of higher missing masses [3,4]. It is therefore reasonable to ask whether a similar approach could not be usefully tried for the low-energy $dd \to {}^4\text{He}\,\pi\pi$ reaction.

The two-step model with an intermediate $pd \to {}^3\text{He}\,\pi^0$ step has in fact been applied successfully to the production of η-mesons in the $dd \to {}^4\text{He}\,\eta$ reaction near threshold [16], where it reproduces reasonably well the magnitude of the total cross-section [17,18]. The approach is here extended in sect. 2 to describe the $dd \to {}^4\text{He}\,\pi\pi$ reaction, using the same $\pi N \to \pi\pi N$ amplitudes as those that worked for $pd \to {}^3\text{He}\,\pi\pi$. The other element that is crucial for the evaluation of this model is the cluster decomposition of the α-particle in terms of ${}^3\text{He}\,n/{}^3\text{H}\,p$ constituents. This is discussed in sect. 3, where we rely on the

[a] e-mail: goran.faldt@tsl.uu.se
[b] e-mail: ulla.tengblad@tsl.uu.se
[c] e-mail: cw@hep.ucl.ac.uk

work of the Argonne group [19]. The results presented in sect. 4 show that the model is capable of describing the shape of the $\pi\pi$ effective mass distribution, without the oscillatory structure predicted by the double-Δ model [12]. However, the total cross-section estimates fall over an order of magnitude below the experimental results found at low energies [6,7,13]. These data have low statistics and limited acceptance, though they will be supplemented by more precise results expected soon from CELSIUS [8]. Since neither this nor the double-Δ model gets even close to the observed production rates, alternative approaches are necessary.

2 The reaction model

The two-step model for the $dd \to {}^4\mathrm{He}\,\pi\pi$ amplitudes, in terms of those for $pd \to {}^3\mathrm{H}\,\pi^+$ and $\pi^+ n \to (\pi\pi)^0 p$, is depicted in fig. 1. Contributions involving intermediate ${}^3\mathrm{He}$ and π^0/π^- are all related to the results for this diagram through isospin invariance. Due to the identical nature of the incident deuterons, there is a similar set of diagrams where the initial production takes place on the upper deuteron.

The cross-section corresponding to such a diagram has been evaluated for the $dd \to \alpha\,\eta$ reaction [16] and we follow closely the techniques used there. The unpolarised $dd \to {}^4\mathrm{He}\,\pi\pi$ differential cross-section is expressed in terms of the Lorentz-invariant matrix element $\mathcal{M}$ through

$$\mathrm{d}\sigma = \frac{p_\alpha}{144 p_d W^2} \frac{1}{(2\pi)^4} \sum_{\mathrm{spins}} |\,\mathcal{M}\,|^2 \; k_{\pi\pi}\,\mathrm{d}m_{\pi\pi}\,\mathrm{d}\Omega_\alpha \frac{\mathrm{d}\Omega_{\pi\pi}}{4\pi}\,. \tag{2.1}$$

Here p_d and p_α are the initial and final momenta in the overall cm system where the total energy is W. The angles Ω_α are also in the total cm system, whereas the $\pi\pi$ relative momentum $k_{\pi\pi}$ and its angles $\Omega_{\pi\pi}$ are evaluated in the dipion rest frame, where the total energy is $m_{\pi\pi}$.

The matrix element of fig. 1 involves the integration of the pion propagator between the two production vertices over the two Fermi momenta $\boldsymbol{k}$ and $\boldsymbol{q}$. If initially we neglect the deuteron D-state and the Lorentz boost of the wave functions, this can be written as

$$\mathcal{M} = \sqrt{\frac{2}{3m_p^2}}\,\frac{1}{(2\pi)^3}\int \mathrm{d}^3k\,\mathrm{d}^3q\,\frac{m_n}{E_n(\boldsymbol{p}_n)}\frac{m_t}{E_t(\boldsymbol{p}_t)}$$
$$\times \frac{i}{q_\pi^2 - m_\pi^2 + i\epsilon}\tilde{\mathcal{M}}_N, \tag{2.2}$$

where the particle masses are denoted by m_i. The reduced nuclear matrix element is

$$\tilde{\mathcal{M}}_N = \mathrm{Tr}\left[\frac{-1}{\sqrt{2}}\,\boldsymbol{\sigma}\cdot\boldsymbol{\epsilon}_d\left\{-\mathcal{A}\,\hat{\boldsymbol{p}}_d\cdot\boldsymbol{\epsilon}_{d'} - i\mathcal{B}\,\hat{\boldsymbol{p}}_d\cdot(\boldsymbol{\epsilon}_{d'}\times\boldsymbol{\sigma})\right\}\right.$$
$$\left.\times \frac{-1}{\sqrt{2}}\,a(m_{\pi\pi}, Q)\,\boldsymbol{\sigma}\cdot\boldsymbol{p}_\pi\right]\tilde{\varphi}_d(\boldsymbol{q})\,\tilde{\psi}_\alpha^\dagger(\boldsymbol{k}), \tag{2.3}$$

where the $(\boldsymbol{\epsilon}_d, \boldsymbol{\epsilon}_{d'})$ are the polarisation vectors of the two incident deuterons and the kinematics are defined as in
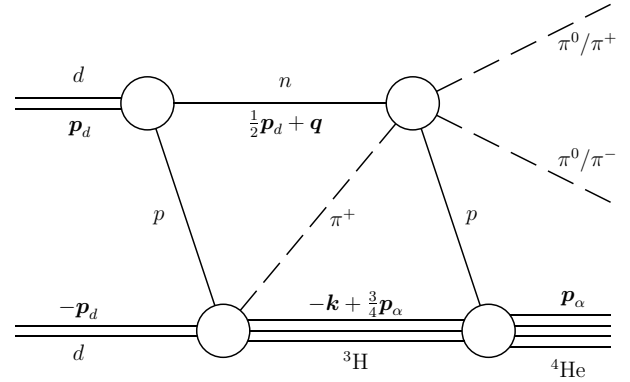

Fig. 1. Two-step model for the production of $\pi^+\pi^-$ and $\pi^0\pi^0$ pairs through the $dd \to {}^4\mathrm{He}\,\pi\pi$ reaction. There are also contributions related to this by isospin in addition to the terms arising from the interchange of the two deuterons.

the figure. The S-state momentum-space wave functions for the deuteron and the triton-proton configuration of the α-particle are denoted by $\tilde{\varphi}_d(\boldsymbol{q})$ and $\tilde{\psi}_\alpha(\boldsymbol{k})$, respectively.

In the forward and backward (cm) directions, only two terms are needed to describe the spin structure of the $dp \to {}^3\mathrm{He}\,\pi^0$ amplitude. Using two-component spinors to denote the ${}^3\mathrm{He}$ (u_h) and proton (u_p), this reads

$$\mathcal{M}(dp \to {}^3\mathrm{He}\,\pi^0) = u_h^\dagger\left[\mathcal{A}\,\hat{\boldsymbol{p}}_d\cdot\boldsymbol{\epsilon}_d + i\mathcal{B}\,\hat{\boldsymbol{p}}_d\cdot(\boldsymbol{\epsilon}_d\times\boldsymbol{\sigma})\right]u_p, \tag{2.4}$$

where $\boldsymbol{p}_d$ and $\boldsymbol{p}_\pi$ are the momenta of the incident deuteron and produced pion, respectively. In our normalisation, the unpolarised differential cross-section and deuteron tensor analysing power t_{20} are given in terms of the two dimensionless spin amplitudes $\mathcal{A}$ and $\mathcal{B}$ by

$$\frac{\mathrm{d}\sigma}{\mathrm{d}\Omega} = \frac{1}{3(8\pi W)^2}\frac{p_\pi}{p_d}\left[\,|\,\mathcal{A}\,|^2 + 2\,|\,\mathcal{B}\,|^2\,\right],$$
$$t_{20} = \sqrt{2}\left[\frac{|\,\mathcal{B}\,|^2 - |\,\mathcal{A}\,|^2}{|\,\mathcal{A}\,|^2 + 2\,|\,\mathcal{B}\,|^2}\right], \tag{2.5}$$

and these observables have been well measured in collinear kinematics at Saturne [20].

For deuteron kinetic energies of interest here, the backward ($\theta_{p\pi} = 180°$) values of t_{20} are strongly negative, so that $|\mathcal{A}| \gg |\mathcal{B}|$. In the 0.5–0.8 GeV range the results may be represented by

$$|\mathcal{A}|^2 \approx -565.6 + 2318.7 T_d - 2869.9 T_d^2 + 1122.9 T_d^3,$$
$$|\mathcal{B}|^2 \approx -197.9 + 1144.9 T_d - 2113.0 T_d^2 + 1261.8 T_d^3, \tag{2.6}$$

where the deuteron kinetic energy T_d is measured in GeV.

The spin structure of the $\pi^- p \to \pi^0\pi^0 n$ amplitude is unique near threshold:

$$M(\pi^- p \to \pi^0\pi^0 n) = a(m_{\pi\pi}, Q)\,u_n^\dagger\,\boldsymbol{\sigma}\cdot\boldsymbol{p}_p\,u_p. \tag{2.7}$$

In terms of the amplitude a, the unpolarised differential cross-section is

$$\mathrm{d}\sigma(\pi^- p \to \pi^0\pi^0 n) = \frac{1}{64\pi^3}\frac{p_p\,p_n}{W_{\pi N}^2}\,|a(m_{\pi\pi}, Q)|^2\,k_{\pi\pi}\,\mathrm{d}m_{\pi\pi}. \tag{2.8}$$

Here, p_p and p_n are, respectively, the initial and final nucleon momenta, $W_{\pi N}$ the cm energy in the πN system, and $Q = W_{\pi N} - 2m_\pi - m_N$ the excess energy above the two-pion threshold.

The low-energy data in different isospin channels are well described by the Valencia model [15] and this allows one to project out the $I = 0$ combination required as input in eq. (2.3). The results can be parameterised as

$$\frac{1}{64\pi^3}|a(m_{\pi\pi}, Q)|^2 = (1.092 - 0.0211Q + 0.00015Q^2)$$
$$+ (4.18 + 0.0075Q - 0.00098Q^2)\, x$$
$$+ (47.65 - 0.935Q + 0.00743Q^2)\, x^2 \, \mu\text{b/MeV}^2, \quad (2.9)$$

where $x = (m_{\pi\pi} - 2m_\pi)/m_\pi$.

Due to small recoil corrections, this parameterisation should be used at an excess energy of Q', where

$$Q' \approx xm_\pi + (Q - xm_\pi)(1 + 2m_\pi/m_\alpha)/(1 + 2m_\pi/m_p). \tag{2.10}$$

Since large Fermi momenta are not required in the two-step model, the $dp \to {}^3\text{He}\,\pi^0$ and $\pi N \to \pi\pi N$ amplitudes can be taken outside of the integration in eq. (2.2) with the values pertaining at zero Fermi momenta. Considering only the positive-energy pion pole, to first order in $\boldsymbol{k}$ and $\boldsymbol{q}$ one is left with a difference between the external and internal energies of

$$\Delta E = E_{\text{ext}} - E_{\text{int}} = \Delta E_0 + \boldsymbol{k} \cdot \boldsymbol{W} + \boldsymbol{q} \cdot \boldsymbol{V}, \tag{2.11}$$

where

$$\Delta E_0 = E_\pi^0 - E_\pi, \tag{2.12}$$

with

$$E_\pi^0 = 2E_d - E_t - E_n - E_\pi. \tag{2.13}$$

Here (E_π, E_d, E_t, E_n) are the pion, deuteron, triton, and nucleon total energies, evaluated, respectively, at momenta $-\frac{3}{4}\boldsymbol{p}_\alpha - \frac{1}{2}\boldsymbol{p}_d$, $\boldsymbol{p}_d$, $\frac{1}{2}\boldsymbol{p}_d$, and $\frac{3}{4}\boldsymbol{p}_\alpha$.

The relativistic relative velocity vectors $\boldsymbol{V}$ and $\boldsymbol{W}$ depend only upon external kinematic variables:

$$\boldsymbol{V} = \boldsymbol{v}_\pi(-\tfrac{3}{4}\boldsymbol{p}_\alpha - \tfrac{1}{2}\boldsymbol{p}_d) - \boldsymbol{v}_n(\tfrac{1}{2}\boldsymbol{p}_d)$$
$$= -\frac{3}{4E_\pi}\boldsymbol{p}_\alpha - \frac{1}{2}\left[\frac{1}{E_\pi} + \frac{1}{E_n}\right]\boldsymbol{p}_d,$$

$$\boldsymbol{W} = -\boldsymbol{v}_\pi(-\tfrac{3}{4}\boldsymbol{p}_\alpha - \tfrac{1}{2}\boldsymbol{p}_d) + \boldsymbol{v}_t(\tfrac{3}{4}\boldsymbol{p}_\alpha)$$
$$= \frac{3}{4}\left[\frac{1}{E_\pi} + \frac{1}{E_t}\right]\boldsymbol{p}_\alpha + \frac{1}{2E_\pi}\boldsymbol{p}_d. \tag{2.14}$$

The resulting form factor

$$\mathcal{S}(\boldsymbol{V}, \boldsymbol{W}, \Delta E_0) =$$
$$-i\int \mathrm{d}^3k\,\mathrm{d}^3q\,\frac{1}{\Delta E_0 + \boldsymbol{k} \cdot \boldsymbol{W} + \boldsymbol{q} \cdot \boldsymbol{V} + i\epsilon}\,\tilde{\psi}^*(\boldsymbol{k})\,\tilde{\varphi}(\boldsymbol{q})$$
$$= (2\pi)^3 \int_0^\infty \mathrm{d}t\, e^{it\Delta E_0}\,\psi^*(-t\boldsymbol{W})\,\varphi(t\boldsymbol{V}), \tag{2.15}$$

then involves a one-dimensional integration over wave functions in configuration space. In terms of this form factor the $dd \to {}^4\text{He}\,\pi\pi$ differential cross-section becomes

$$\mathrm{d}\sigma = \frac{N_\alpha}{48\,(2\pi)^{10}}\frac{p_\alpha p_d}{[m_p W(E_\pi + E_\pi^0)]^2}\,|a(m_{\pi\pi}, Q)|^2$$
$$\times |\mathcal{S}(\boldsymbol{V}, \boldsymbol{W}, \Delta E_0) + (\boldsymbol{p}_d \Leftrightarrow -\boldsymbol{p}_d)|^2$$
$$\times \left\{|\,\mathcal{A}\,|^2 + 2\,|\,\mathcal{B}\,|^2\right\}\,k_{\pi\pi}\,\mathrm{d}m_{\pi\pi}\mathrm{d}\Omega_\alpha, \tag{2.16}$$

where N_α is the normalisation of the ^{4}He wave function and the extra form-factor contribution coming from the interchange of the two incident deuterons is indicated. All isospin factors have been included, but it must be stressed that in eq. (2.16) $\mathcal{A}$ and $\mathcal{B}$ refer to the $dp \to {}^3\text{He}\,\pi^0$ and $\pi^- p \to \pi^0\pi^0 n$ charge states, respectively. Isospin invariance dictates that $\pi^+\pi^-$ production in $dd \to {}^4\text{He}\,\pi\pi$ should be a factor of two larger than $\pi^0\pi^0$, but this simple rule is significantly modified near threshold by phase space factors arising from the pion mass difference.

Two further refinements need to be implemented in eq. (2.16) before comparing its predictions with experiment. Although the final α-particle is slow in the cm system, relativistic corrections cannot be neglected for the incident deuterons. These can be included by boosting $V_\parallel$, the longitudinal component of $\boldsymbol{V}$, *i.e.* by taking as argument of the deuteron wave function [16]

$$\boldsymbol{V}' = (\boldsymbol{V}_\perp,\, E_d V_\parallel/m_d). \tag{2.17}$$

Secondly, the effects of the deuteron D-state have to be considered and this can be accomplished by introducing two form factors:

$$\mathcal{S}_{S,D}(\boldsymbol{V}', W, \Delta E_0)$$
$$= 2\pi^2 \int_0^\infty \mathrm{d}t\, e^{it\Delta E_0}\,\Psi^*(-tW)\,\Phi_{S,D}(t\boldsymbol{V}'), \tag{2.18}$$

where $\Phi_{S,D}(r)$ are the deuteron S- and D-state configuration space wave functions normalised by

$$\int_0^\infty r^2\left\{\Phi_S(r)^2 + \Phi_D(r)^2\right\}\mathrm{d}r = 1. \tag{2.19}$$

The S- and D-state form factors enter in different combinations for the $\mathcal{A}$ and $\mathcal{B}$ amplitudes and, after making kinematic approximations in respect of the D-state combined with the Lorentz boost, one finds

$$\mathrm{d}\sigma = \frac{N_\alpha}{48\,(2\pi)^{10}}\frac{p_\alpha p_d}{[m_p W(E_\pi + E_\pi^0)]^2}\,|a(m_{\pi\pi}, Q)|^2\,k_{\pi\pi}$$
$$\times \left\{|\,\mathcal{A}\,|^2\left|\mathcal{S}_S(V', W, \Delta E_0) - \sqrt{2}\,\mathcal{S}_D(V', W, \Delta E_0)\right|^2\right.$$
$$\left. + 2\,|\,\mathcal{B}\,|^2\left|\mathcal{S}_S(V', W, \Delta E_0) + \frac{1}{\sqrt{2}}\,\mathcal{S}_D(V', W, \Delta E_0)\right|^2\right\}$$
$$\times \mathrm{d}m_{\pi\pi}\,\mathrm{d}\Omega_\alpha, \tag{2.20}$$

where, as in eq. (2.16), it is assumed that contributions from form factors resulting from the interchange $\boldsymbol{p}_d \Leftrightarrow -\boldsymbol{p}_d$ have been included.
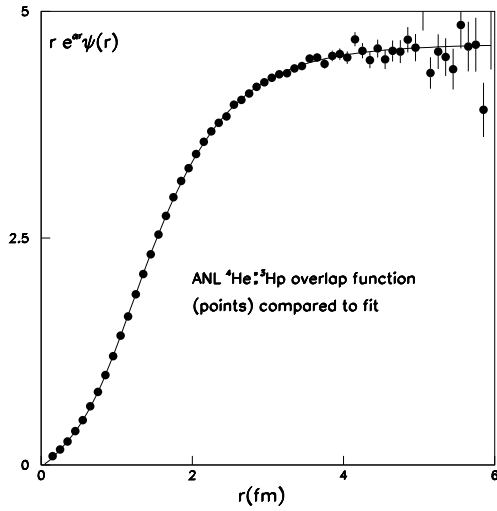
Fig. 2. Unnormalised ^{4}He : ^{3}H p overlap function as a function of the ^{3}H-p separation distance. For the purposes of presentation, this has been multiplied by $r\,\mathrm{e}^{\alpha r}$, where the charge average $\alpha = 0.854\,\mathrm{fm}^{-1}$. The results of ref. [19] have been parameterised as in eq. (3.1).

3 The ^{4}He wave function

Over the last few years there has been remarkable progress in *ab initio* calculations of the structure of light nuclei using variational Monte Carlo techniques [19]. Starting from realistic nucleon-nucleon potentials, it has been possible to identify various cluster sub-structures in nuclei as heavy as ^{9}Be. The results for the unnormalised ^{4}He : ^{3}H p overlap function in configuration space are shown in fig. 2, where the error bars arise from the sampling procedure.

The overlap function has been parameterised by

$$\psi(r) = \sqrt{N_\alpha}\,\frac{1}{r}\sum_{n=1}^{6} a_n\,\mathrm{e}^{-n\alpha r}, \qquad (3.1)$$

where $\alpha = 0.854\,\mathrm{fm}^{-1}$ represents the average for the ^{3}H p and ^{3}He n configurations. To ensure good behaviour at the origin, the final parameter is fixed by $a_6 = -\sum_{n=0}^{5} a_n$, while the other values are sequentially 5.1525, -2.8414, -45.1886, 110.7401, and -100.3994. The normalisation has been chosen such that

$$\int_0^\infty r^2\,[\psi(r)]^2\,\mathrm{d}r = N_\alpha. \qquad (3.2)$$

In the spirit of our approach here to pion production, where only these cluster contributions are considered, it is appropriate to assume that the $p\,^3$H and $n\,^3$He components saturate the wave function and take $N_\alpha = 4$ rather than the reduced spectroscopic factor obtained in ref. [19].

4 Results and conclusions

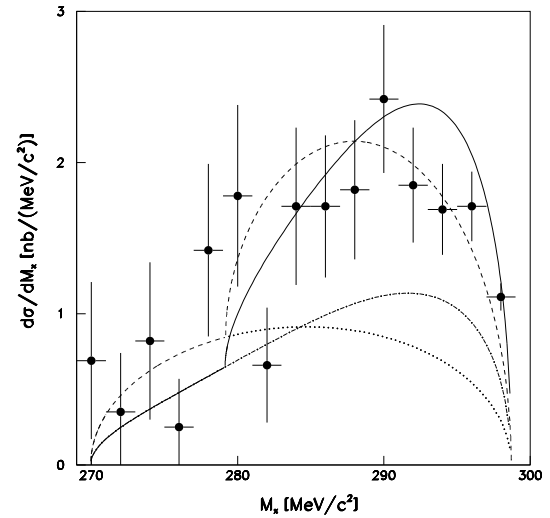In fig. 3 we show the prediction of the shape of the missing-mass distribution for inclusive two-pion production at an

Fig. 3. Missing-mass distribution for the $dd \to\,^4$He X reaction measured at 570 MeV [6]. The chain curve corresponds to $\pi^0\pi^0$ production within the two-step model, whereas the solid one represents the sum of this and $\pi^+\pi^-$ production. The predictions are normalised to the integrated cross-section by multiplying by a factor of 17.6. The dotted and broken curves are the similar predictions from phase space, again normalised to the total rate.

excess energy of $Q = 29\,\mathrm{MeV}$ with respect to the $2\pi^0$ threshold. Though the general form is in good agreement with the experimental data [6,7], the results are too low by almost a factor of twenty! The peak of the distribution is predicted to be a little to the right of that corresponding to pure phase space, which is also shown. Such a feature was clearly observed for the $pd \to\,^3$He $\pi\pi$ reaction at low energies [14], but the limited statistics in the dd case prevents us from drawing firm conclusions here. Estimates in the double-Δ model [12], which agreed convincingly with the data in the resonance region, were even poorer compared to the near-threshold data. Apart from being a similar factor of twenty too low, this model also predicted significant structure in the mass distribution which is absent from the experimental data.

The discrepancy is similar for the other low-energy data [13], though here the acceptance was small and assumptions had to be made in order to extract a total cross-section. In fig. 4 we show the estimates of the total cross-sections for the production of charged and neutral pions within the two-step model.

The central problem for any model that attempts to describe the $dd \to\,^4$He $\pi\pi$ cross-section at low energies is that the production of isoscalar pion pairs is of a similar magnitude in deuteron-deuteron and proton-deuteron collisions. Extrapolating the $I = 0$ $pd \to\,^3$He $\pi\pi$ cross-section of ref. [4] from $Q = 37\,\mathrm{MeV}$ down to 29 MeV, where the $dd \to\,^4$He $\pi\pi$ cross-section was measured [6], assuming a phase space Q^2 behaviour, we see that

$$\frac{\sigma_{\mathrm{tot}}(dd \to\,^4\mathrm{He}\,\pi\pi)}{\sigma_{\mathrm{tot}}(pd \to\,^3\mathrm{He}\,\pi\pi)} \approx \frac{40\,\mathrm{nb}}{70\,\mathrm{nb}} = \frac{4}{7}\,. \qquad (4.1)$$

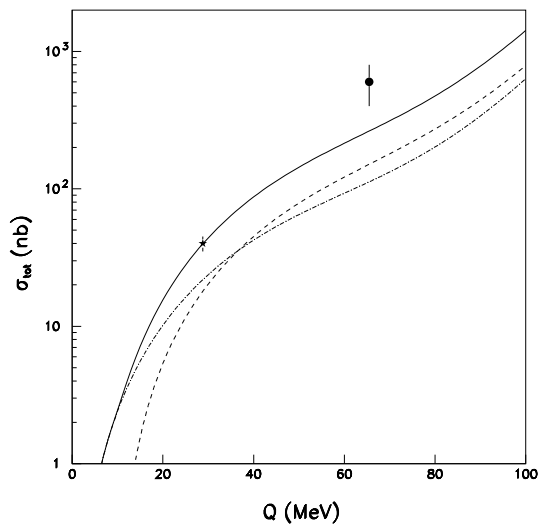**Fig. 4.** Total cross-section for the $dd \to$ ^{4}He $\pi\pi$ reaction. The experimental data from ref. [6] (star) and ref. [13] (circle) are compared to the predictions of the two-step model scaled by a factor of 17.6. The chain curve corresponds to $\pi^0\pi^0$ production, the broken to $\pi^+\pi^-$, and the solid to their sum.

On the other hand, the production of the η-meson is much weaker in the dd case, with the ratio of the squares of the amplitudes being [17,18,21,22]

$$\frac{\left|f(dd \to {}^4\text{He}\,\eta)\right|^2}{\left|f(pd \to {}^3\text{He}\,\eta)\right|^2} \approx \frac{1}{50}, \qquad (4.2)$$

though perhaps this would be increased by a factor of two if corrections were made for the effects of the η-nucleus final-state interaction. Since the low-energy $pd \to$ ^{3}He $\pi\pi$, $pd \to$ ^{3}He η, and $dd \to$ ^{4}He η cross-sections are all successfully described by the two-step model, one might therefore expect to undershoot the $dd \to$ ^{4}He $\pi\pi$ total cross-section by a factor of $50 \times 4/7 \approx 30$ in such a model. This is to be compared to the 17.6 used to fit the data in fig. 4. However, orders-of-magnitude comparisons of the type made here do not take into account fully the spin-parity considerations. For example, the $dd \to$ ^{4}He $\pi\pi$ prediction would be increased by more than a factor of two if the sign of the deuteron D-wave were arbitrarily reversed in eq. (2.20).

Given that neither the two-step nor the double-Δ model seems capable of describing the magnitude of the $dd \to$ ^{4}He $\pi\pi$ cross-section near threshold, one must seek alternative explanations or modifications to the existing mechanisms. Other diagrams, such as that of the impulse approximation where the process is driven by $pd \to$ ^{3}He $\pi\pi$ with a spectator nucleon, give very small cross-sections due to the large momentum transfer. We have not included any specific $\pi\pi$ final-state interaction, but the s-wave scattering lengths are relatively small [23] and, in any case, the effects are implicitly included through the use of empirical $\pi N \to \pi\pi N$ amplitudes [15].

The interaction of the low-energy pions with the final ^{4}He nucleus might enhance the cross-section since it is known that the p-wave pion-nucleus interaction is attractive near threshold [24]. However, the effect will steadily diminish with energy and eventually change sign at the resonance. Crude estimates indicate that any effects due to such final-state interactions are likely to be less than 50%, even very close to threshold, and so they are very unlikely to provide the explanation of the defect.

Now, although we have normalised the ^{4}He wave function as if it consisted purely of $p\,^3\text{H}/n\,^3\text{He}$ pairs, in reality the ^{3}H in such a nucleus is on average smaller than the physical triton. Nevertheless, we have taken the amplitudes for $pd \to$ ^{3}He π^0 from the measured data. The same criticism can be levelled at the double-Δ model, where the final deuteron in the $pp \to d\pi^+$ input would really be required for a *small* deuteron. If there were major corrections due to such effects they would be likely to be present at all energies and hence destroy the excellent agreement with data achieved at higher energies [12]. Further inspiration is therefore clearly needed to resolve this dilemma.

References

1. S. Prakhov *et al.*, Phys. Rev. C **69**, 045202 (2004).
2. W. Brodowski *et al.*, Phys. Rev. Lett. **88**, 192301 (2002).
3. F. Belleman *et al.*, Phys. Rev. C **60**, 61002 (1999).
4. M. Andersson *et al.*, Phys. Lett. B **485**, 327 (2000).
5. M. Bashkanov *et al.*, Phys. Lett. B **637**, 223 (2006).
6. C. Bargholtz *et al.*, Phys. Lett. B **398**, 264 (1997).
7. P. Thörngren Engblom, PhD Thesis, University of Stockholm, 1997.
8. P. Thörngren Engblom, TSL proposal C65 (under analysis).
9. A. Abashian, N.E. Booth, K.M. Crowe, Phys. Rev. Lett. **5**, 258 (1960).
10. J. Banaigs *et al.*, Nucl. Phys. B **67**, 1 (1973).
11. R. Wurzinger *et al.*, Phys. Lett. B **445**, 423 (1999).
12. A. Gårdestig, G. Fäldt, C. Wilkin, Phys. Rev. C **59**, 2608 (1999).
13. K.R. Chapman *et al.*, Phys. Lett. **21**, 465 (1966).
14. G. Fäldt, A. Gårdestig, C. Wilkin, Phys. Lett. B **496**, 185 (2000).
15. M.J. Vicente Vacas, E. Oset, Phys. Rev. C **60**, 064621 (1999).
16. G. Fäldt, C. Wilkin, Nucl. Phys. A **596**, 488 (1996).
17. R. Frascaria *et al.*, Phys. Rev. C **50**, 537 (1994).
18. N. Willis *et al.*, Phys. Lett. B **406**, 14 (1997).
19. J.L. Forest *et al.*, Phys. Rev. C **54**, 646 (1996), but see also the important updates reported in http://www.phy.anl.gov/theory/research/overlap.
20. C. Kerboul *et al.*, Phys. Lett. B **181**, 28 (1986).
21. J. Berger *et al.*, Phys. Rev. Lett. **61**, 919 (1988).
22. B. Mayer *et al.*, Phys. Rev. C **53**, 2068 (1996).
23. J.R. Batley *et al.*, Phys. Lett. B **633**, 173 (2006).
24. See for example, T.E.O. Ericson, W. Weise, *Pions and Nuclei* (OUP, Oxford, 1988).